Article

Applied Spectroscopy

Applied Spectroscopy
0(0) 1–7

DOI: 10.1177/0003702819848501
journals.sagepub.com/home/asp
SAGE

Two-Dimensional Correlation Spectroscopy (2D-COS) Studies of Solution Mixtures in the Low Frequency Raman Region

Shuyu Xu[1], D. Bruce Chase[1], John F. Rabolt[1], and Isao Noda[1,2]

Abstract

Raman spectra of a series of binary solution mixtures, including chloroform ($CHCl_3$), ethanol (EtOH), and 1,1,1,3,3,3-hexafluoro-2-propanol (HFIP), were analyzed using the two-dimensional correlation spectroscopic (2D-COS) technique in the low frequency region. Numerous asynchronous cross-peaks ubiquitously appeared in the concentration-dependent Raman spectra of these organic solvent mixtures. The result clearly demonstrated a deviation from ideal solution behavior, reflecting the presence of specific molecular interactions causing a subtle nonlinear spectral intensity response of Raman bands to the concentration changes. Furthermore, the combination of 2D-COS and low frequency Raman spectroscopy was extended to poly[(R)-3-hydroxybutyrate-*co*-(R)-3-hydroxyhexanoate] (PHBHx) copolymer solutions in $CHCl_3$-HFIP co-solvents. The results suggest the existence of hydrogen bonding interaction between the PHBHx and HFIP, which is consistent with the previous infrared spectroscopic study of PHBHx solutions.

Keywords

Low frequency Raman spectroscopy, two-dimensional correlation spectroscopy, 2D-COS, organic solvent mixtures, PHBHx random copolymers

Date received: 5 February 2019; accepted: 9 April 2019

Introduction

Signals arising from the low frequency Raman region can provide molecular conformational information and insight into the interaction of chains in a crystal. The spectral modes observed in this region originate from weak bonds, translational and rotational lattice modes in ordered solids, intrachain accordion modes, etc.[1] However, Raman spectra specific to the low frequency region have not been readily accessible on current Raman instruments for the last 20 years until the recent development of volume holographic grating (VHG) techniques.[2] Due to VHG, the strong elastic Rayleigh scattering can be largely suppressed, allowing the subtle molecular information carried in the low frequency Raman modes to become observable. The analysis of low frequency Raman vibrations of materials has now been applied extensively to polymeric, pharmaceutical, forensics, and especially for the identification of polymorphic structures during the crystallization process.[3–5] The low frequency Raman modes of polymorphic structures of crystals are not only very distinguishable from each other, but also can be much more intense compared to that of higher frequency Raman modes.

In addition, two-dimensional correlation spectroscopy (2D-COS) has been shown to be a useful technique for analysis of spectra from materials under perturbation, such as temperature, pressure, systematic change in the concentration of mixtures, and so on. It is well known that 2D-COS enhances the resolution of spectra by spreading the spectral features along the second dimension. Two-dimensional COS spectra consist of two orthogonal parts. The synchronous correlation spectrum indicates how similarly separate peaks change under the perturbation, either in the same direction or in opposite ways. In contrast, the asynchronous correlation spectrum is a measure

[1]Department of Materials Science and Engineering, University of Delaware, Newark, DE, USA
[2]Danimer Scientific, Bainbridge, GA, USA

Corresponding author:
Isao Noda, University of Delaware, 201 DuPont Hall, Newark, DE 19716-3106, USA.
Email: noda@udel.edu

of out-of-phase changes in peak signals under the given perturbation, which is a measure of the intensity changes among the peaks occurring in sequence instead of simultaneously. The detailed interpretation rules of 2D-COS have been reviewed extensively in the literature.[6–10]

In general, mixtures of two liquids are often entirely miscible in all proportions to give a single liquid solution. $CHCl_3$ and EtOH, for example, can be mixed at any arbitrary ratio to form a single solution. For an ideal solution mixture, the molecular interactions between the constituents are concentration-independent; macroscopic properties of the mixture, such as volume and vapor pressure, are strictly proportional to the composition of components in the pure state. In this work, we re-examined the ideal nature of several pairs of simple binary solvent mixtures, such as $CHCl_3$–EtOH and toluene–EtOH, in the low frequency Raman region by applying 2D-COS analysis. If a binary mixture behaves as an ideal solution, spectral changes in the intensity variations must be synchronized; therefore, no cross-peak in the asynchronous 2D correlation spectrum should be expected. We have also extended the analysis of 2D-COS into the low frequency Raman spectral region of PHBHx solution in $CHCl_3$–HFIP co-solvent system, which elucidated subtle interactions between PHBHx and HFIP.

Experimental

Materials and Sample Preparation

Poly[(R)-3-hydroxybutyrate-*co*-(R)-3-hydroxyhexanoate] copolymer was supplied by the Procter and Gamble Company (Cincinnati, OH, USA), with 3.9 mol% Hx content, $M_w = 843\,000$ g/mol, and PDI = 2.2. All the other chemicals were purchased from Sigma-Aldrich and were used as received with no further purification. The samples of binary organic mixtures were prepared at various combinations of concentrations. Binary mixtures of $CHCl_3$ and EtOH ($CHCl_3$–EtOH), for instance, were prepared with increasing molar fraction of $CHCl_3$, denoted as n_C, from pure EtOH ($n_C = 0$) to pure $CHCl_3$ ($n_C = 1.0$). As for the preparation of polymer solutions, 10 wt% PHBHx was dissolved in $CHCl_3$–HFIP co-solvents at different molar fractions of HFIP, from pure $CHCl_3$ ($n_H = 0$) to 10 mol% HFIP in $CHCl_3$–HFIP ($n_H = 0.1$). The polymer solutions were kept at room temperature and stirred overnight to insure a thorough dissolution of the PHBHx. The preparation and denotation of other organic solvent mixtures followed a similar description and recipe as stated above.

Raman Measurements and Two-Dimensional Correlation Spectroscopy Analysis

The Raman spectra were recorded using a Kaiser Holospec1.8 Raman Spectrograph (Kaiser Optical Systems, Inc.) equipped with a TE cooled Andor charge-coupled device detector (Oxford Instruments) and an Ondax XLF-CLM probe head and 785 nm laser (Ondax, now a part of Coherent, Inc.). The Raman instrument had a numerical aperture of 0.9 with a magnification of 65×. This instrumental arrangement allowed access to Raman frequencies as low as 10 cm^{-1}. The Raman spectra were recorded using 785 nm excitation with approximately 84 mW laser power and a 30 s exposure. The 2D-COS analysis was executed using the 2D-Shige software developed by Shigeaki Morita (Osaka Electro-Communication University).

Results and Discussion

Binary Solvent Mixtures

The binary mixtures of chloroform and ethanol were first investigated because chloroform is a good solvent for many polyesters. In contrast, ethanol can be a rather poor solvent for these polymers at room temperature. Hence, the mixture of chloroform and ethanol is a convenient pair of co-solvents that can control the precipitation and subsequent crystallization process of polymers. The Raman spectra of $CHCl_3$–EtOH mixtures at various molar ratios of $CHCl_3$ to EtOH were obtained and are shown for both the "fingerprint" (Fig. 1a) and low frequency region (Fig. 1b), respectively. With increasing molar fraction of $CHCl_3$ (n_C) in the $CHCl_3$–EtOH mixture, the intensities of the $CHCl_3$ peaks gradually increased, while those of EtOH correspondingly decreased. The intensity of the $–CCl_3$ stretching vibration of the $CHCl_3$, for instance, showed a seemingly linear relationship as a function of n_C (Fig. 1c). At first glance, this linear dependence of the Raman intensities upon the concentration could be easily considered as a sign of ideal solution behavior with no intermolecular interactions within the $CHCl_3$–EtOH mixtures. Later we will show that is not the case in the 2D-COS studies.

In the low frequency Raman spectra of $CHCl_3$–EtOH, a broad peak centered ~20 cm^{-1}, which dominates this so-called Rayleigh wing region, appeared with increasing n_C. Although Rayleigh scattering was effectively blocked by the VHG notch filters at very low Raman frequencies (<10 cm^{-1}), the presence of the broad Rayleigh wing, reaching approximately 100 cm^{-1}, hindered the further spectral interpretation of this low Raman band. The Rayleigh wing features stem from the various contributions of the relaxational effects. They include the diffusional rotation of molecules, which sometimes results in a profile approximated by a Lorentzian peak centered at the Rayleigh line. To minimize the large interference from the diffusional rotation of molecules dominating the low frequency Raman region, a Lorentzian peak can be constructed for subtraction by using the intensities of two

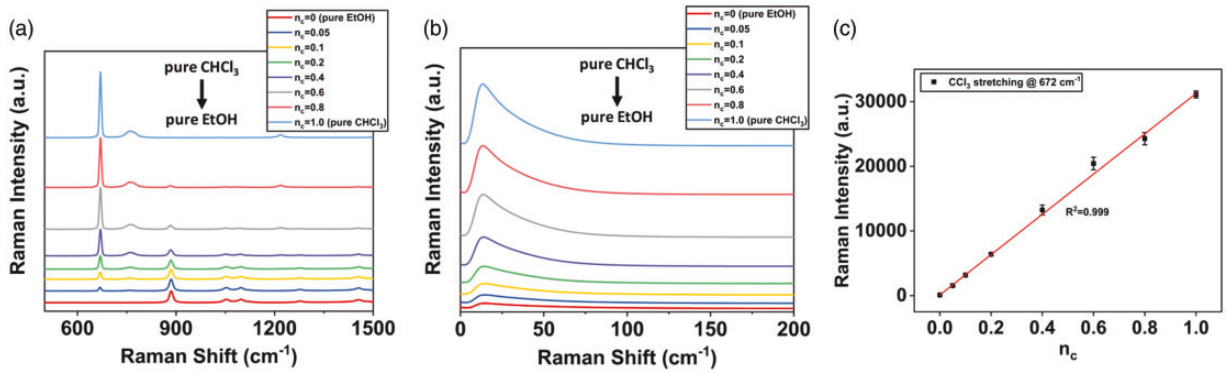

Figure 1. The Raman spectra of $CHCl_3$–EtOH mixtures with n_C increasing from 0 to 1 in (a) the "fingerprint" region of 500–1500 cm^{-1} and (b) the low frequency region of 0–200 cm^{-1}. (c) Raman intensity of $-CCl_3$ stretching at 672 cm^{-1} as a function of n_C.

selected data points, for instance 25 cm^{-1} and 35 cm^{-1}, and removed from the raw spectrum.

To extract the subtle molecular information from the low frequency Raman spectra, two steps of pre-processing of the raw spectra were carried out before 2D-COS analysis: (1) the subtraction of a Lorentzian peak from the spectrum to remove the contribution from diffusional rotation of molecules; and (2) the spectrum obtained from (1) was then used to calculate the so-called reduced Raman spectrum as defined below to further remove the thermal population effects, instrument response, and the effects of the fourth power dependence of scattering on the frequency.[11–13]

$$R(\Delta\tilde{\nu}) = I(\Delta\tilde{\nu}) \cdot (\tilde{\nu}_{laser} - \Delta\tilde{\nu})^{-4} \cdot \Delta\tilde{\nu} \left[1 - \exp\left(-\frac{hc\Delta\tilde{\nu}}{k_B T}\right)\right] \quad (1)$$

$R(\Delta\tilde{\nu})$ and $I(\Delta\tilde{\nu})$, respectively, refer to the reduced intensity and measured Raman intensity of a Raman peak at $\Delta\tilde{\nu}$, $\tilde{\nu}_{laser}$ is the frequecy of the laser excitation, h, c, k_B, and T represent Planck's constant, the velocity of light, the Boltzmann constant and temperature, respectively. The reduced Raman spectra of $CHCl_3$–EtOH and toluene–EtOH with various concentration combinations were calculated and are shown in Fig. 2a and 2b, respectively.

Compared with the raw spectra, more features appeared in the reduced Raman spectra of $CHCl_3$–EtOH. The peak center shifted to ~50 cm^{-1} after removal of the Rayleigh wing contribution. In addition, a weak and broad peak began to appear above 100 cm^{-1} at $n_C = 1.0$. As for the low frequency Raman peaks of toluene–EtOH mixtures, a clear difference was found from that of $CHCl_3$–EtOH. There are two peaks observed at ~75 cm^{-1} and 220 cm^{-1}, with an increase in the molar fraction, n_t, of toluene. Computational calculation, such as density function theory (DFT), would indeed further specify the assignments of the low frequency Raman modes, but it is beyond the scope of this article. To resolve the peaks in the low frequency region and correlate these low frequency signals with regular Raman signals, the reduced Raman spectra of $CHCl_3$–EtOH and toluene–EtOH were further analyzed using 2D-COS.

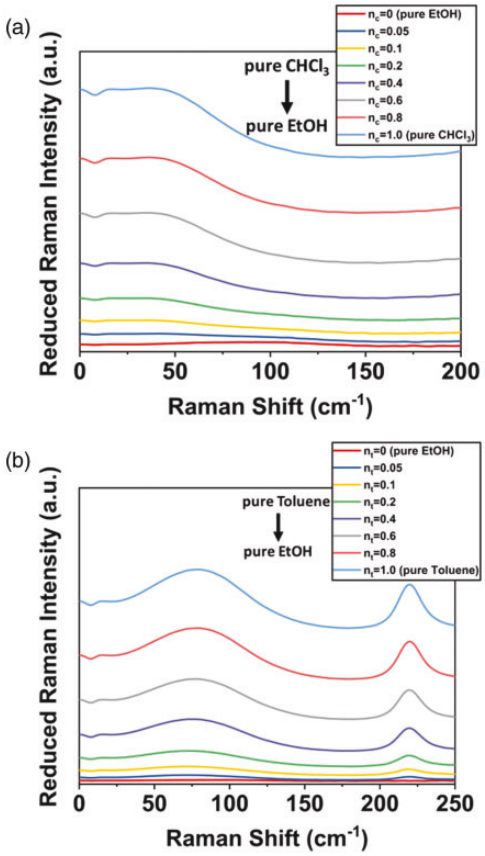

Figure 2. Reduced Raman spectra of (a) $CHCl_3$–EtOH and (b) toluene–EtOH in the low frequency region.

Based on the interpretation rules of 2D-COS, for a truly ideally mixed binary solution where the solvents are

thoroughly miscible, and no concentration-dependent interaction exists, no cross-peaks should be observed in the asynchronous 2D-COS. However, a number of asynchronous peaks were seen in the $CHCl_3$–EtOH (Fig. 3a, lower panel). The existence of the asynchronous signals revealed some deviations from the ideal solution mixture behavior. These deviations could stem from the difference that the molecules of one species (e.g., $CHCl_3$) interacting with the identical species from that interacting with the other species (e.g., EtOH) in the surrounding solution, which

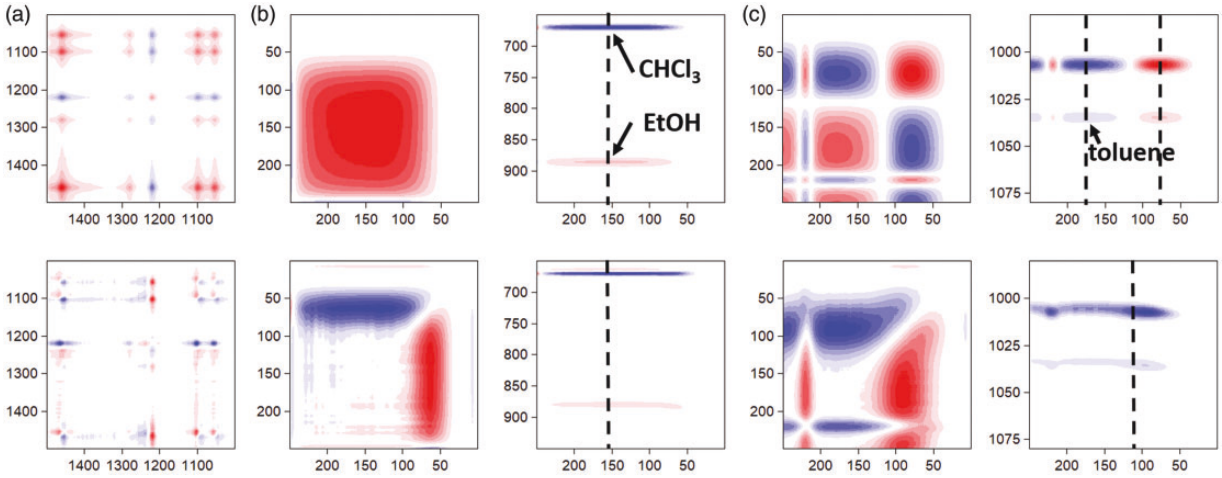

Figure 3. Two-dimensional COS synchronous (upper row) and asynchronous (lower row) spectra of $CHCl_3$–EtOH in (a) the regular Raman region and (b) the low frequency Raman region. (c) Two-dimensional COS synchronous (upper row) and asynchronous (lower row) spectra of toluene–EtOH in the low frequency Raman region.

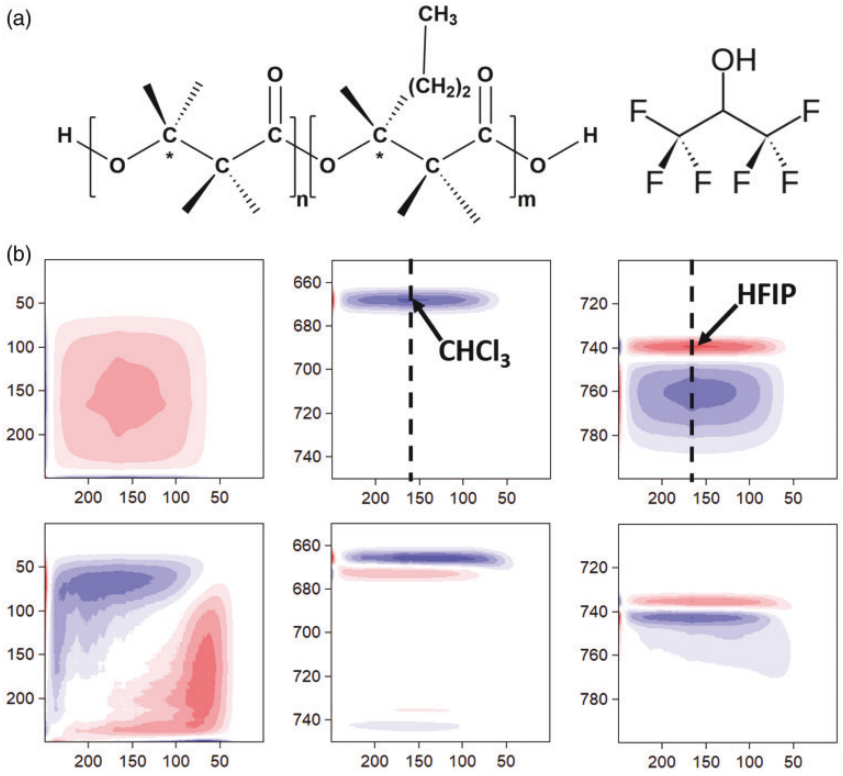

Figure 4. (a) Molecular structure of PHBHx (left) and HFIP (right). (b) Two-dimensional COS synchronous (upper) and asynchronous (lower) spectra of $CHCl_3$–HFIP solvent mixtures.

resulted in the difference, in which the response occurs at higher concentrations, as shown in Fig. 3a. It should be noted that handling moderately unevenly collected spectra as if they are under a fixed increment, as conducted in this study, actually generates results essentially with no adverse effect. Signs and basic appearance of cross-peaks are the same, but the magnitude is slightly modified.[10,14]

Applying 2D-COS analysis in the low frequency Raman region provided more details. A low frequency mode was found at $\sim$150 cm^{-1} in the 2D-COS of $CHCl_3$–EtOH (Fig. 3b), which indicated the presence of subtle molecular interactions. The hetero-mode 2D correlation between the low frequency with regular Raman regions further illustrated that this concentration-dependent molecular interaction was correlated with ethanol. This result could be due to the restricted translation existing among the ethanol molecules.[12,15,16] Similarly, out-of-phase peak intensity changes also existed in the asynchronous 2D-COS of the toluene–EtOH system, demonstrating again that deviations from an ideal solvent mixture behavior exist (Fig. 3c). In addition to a low frequency mode synchronous with EtOH at $\sim$170 cm^{-1}, several more peaks were observed in the 2D-COS of toluene–EtOH. Also, there were two more peaks synchronous to toluene. One was at $\sim$220 cm^{-1}, while the other one was at $\sim$80 cm^{-1}, with the latter being tentatively assigned to the rotatory mode of toluene.[11,17] As demonstrated, 2D-COS has unambiguously provided enhanced spectral resolution to reveal subtle interactions existed in binary solutions.

PHBHx in HFIP–$CHCl_3$

PHBHx is a novel type of bio-produced, biodegradable polymer (Fig. 4a, left).[18] Previous infrared (IR) spectroscopic studies in our group have found that both $CHCl_3$ and HFIP are good solvents for PHBHx. However, the

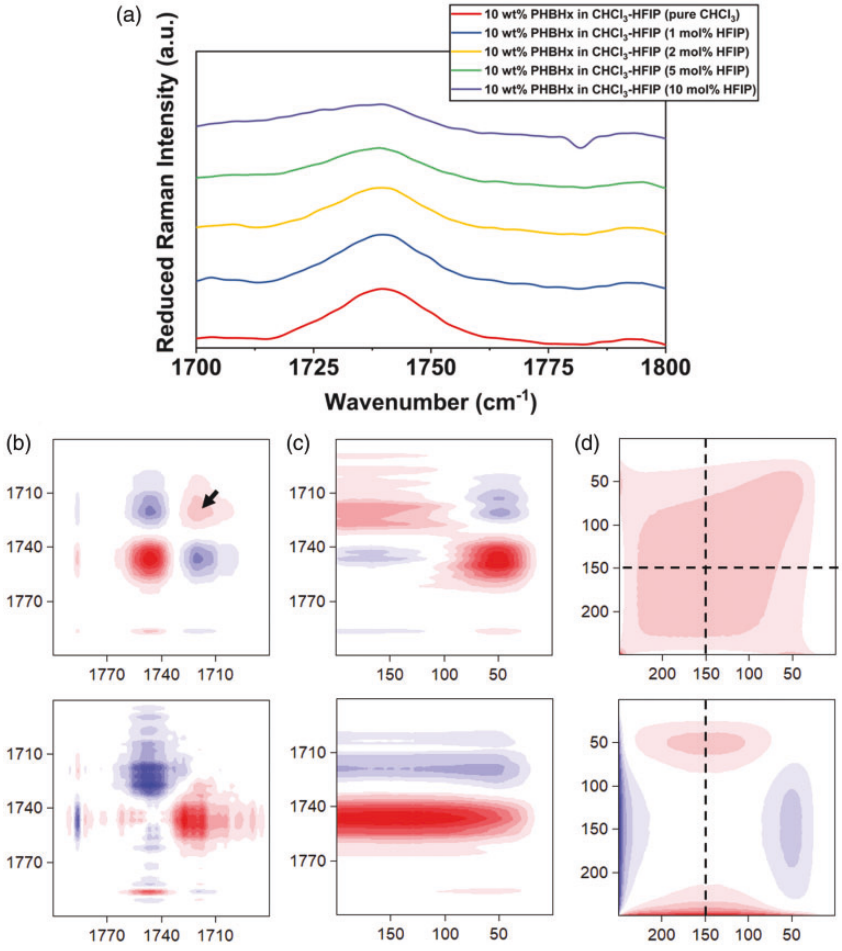

Figure 5. (a) Reduced Raman spectra in the carbonyl region of 10 wt% PHBHx in $CHCl_3$–HFIP co-solvent, from pure $CHCl_3$ to 10 mol% HFIP in $CHCl_3$–HFIP. (b–d) Two-dimensional COS synchronous (upper) and asynchronous (lower) spectra of 10 wt% PHBHx in $CHCl_3$–HFIP co-solvent in (b) the carbonyl region, (c) the low frequency region heterogeneously correlated with carbonyl region, and (d) the low frequency region.

carbonyl stretching band of PHBHx in HFIP solution shifted to lower frequency ~1720 cm^{-1} compared to PHBHx in the $CHCl_3$, where the band is found at ~1740 cm^{-1}. The low frequency band at approximately 1720 cm^{-1} is also observed in the α-crystalline form of solid PHBHx. In fact, this band is often used as the indication of crystal formation in PHBHx. Interestingly, a shift of the carbonyl group was also found for the chemically synthesized atactic homopolymer, poly(3-hydroxybutyrate) (aPHB) in the HFIP solution, which cannot form crystals.[19] Thus, the shift of the carbonyl vibration of PHBHx in HFIP did not result from PHBHx crystal growth in the HFIP. We therefore proposed that this shift was due to the hydrogen bond formed between the hydroxyl group of HFIP interacting with the oxygen in the carbonyl. The strong electronegativity of fluorine in the HFIP makes its hydroxyl hydrogen more acidic.

As shown in the 2D-COS of $CHCl_3$–HFIP mixtures in the low frequency region, a mode at ~160 cm^{-1} was found synchronous with HFIP but asynchronous with $CHCl_3$ (Fig. 4b). Since similar peaks are found in the $CHCl_3$–EtOH and toluene–EtOH mixtures, we hypothesize that this restricted translational mode at ~160 cm^{-1} is related to the hydrogen bonded network formed between the alcohol molecules.

We also studied the PHBHx solution with $CHCl_3$–HFIP co-solvents with increasing HFIP concentration (Fig. 5a). The results showed that, by increasing HFIP concentration in the PHBHx/$CHCl_3$–HFIP solutions from 0 up to 10 mol%, the peak at ~1720 cm^{-1} could be resolved in the 2D-COS of Fig. 5b. This observation indicated a gradual increase of the peak at ~1720 cm^{-1} and a decrease of the peak at ~1740 cm^{-1} with increasing HFIP content. When the carbonyl stretching region was correlated with low frequency Raman peaks in the hetero-mode 2D-COS of Fig. 5c, the low frequency vibration at 150 cm^{-1} was found to be synchronous to the carbonyl peak of PHBHx at 1720 cm^{-1}. Since the peak at 150 cm^{-1} was related to the hydrogen bonding in solution, the synchronization of hydrogen bonds and the carbonyl group at 1720 cm^{-1} could be supportive of the formation of hydrogen bonding between the hydroxyl group of HFIP and the carbonyl group of PHBHx. This result is consistent with our IR observations. Interestingly, the low frequency Raman mode of the hydrogen bonded network in PHBHx/$CHCl_3$–HFIP solution, centered at 150 cm^{-1}, is slightly lower than that in the $CHCl_3$–HFIP co-solvent, which is found at approximately 160 cm^{-1}. This difference could be explained if the carbonyl groups of PHBHx are partially replacing the hydroxyl group of HFIP to from the hydrogen bonded network in the solution. Since the electronegativity of the oxygen in the carbonyl group of PHBHx is weaker than that of the oxygen in the hydroxyl group of HFIP, the Raman mode of the hydrogen bonded network could shift to the lower frequency, from 160 cm^{-1} to 150 cm^{-1}, as shown from the spectral data.

Conclusion

Application of 2D-COS to low frequency Raman spectra can be a very powerful tool to study subtle molecular interactions at high resolution. By using these two techniques, we have demonstrated the existence of deviations from the ideal solution behavior in simple binary organic solvent mixtures, such as $CHCl_3$–EtOH. In addition, the hetero-mode 2D-COS of PHBHx/$CHCl_3$–HFIP solution revealed a low frequency mode of HFIP at ~160 cm^{-1}, which could be correlated to the carbonyl peak of PHBHx at ~1720 cm^{-1}. This low frequency mode was assigned to the hydrogen bonded network in the HFIP and suggested the formation of hydrogen bonding between the HFIP and PHBHx that blue shifted the carbonyl group of PHBHx from ~1740 cm^{-1} to ~1720 cm^{-1}.

Conflict of Interest

The authors report there are no conflicts of interest.

Funding

This work was supported by Delaware NSF EPSCoR Grant no. 1301765 and the NSF DMR Polymers Program Grant DMR-1407255.

ORCID iD

Isao Noda https://orcid.org/0000-0002-0081-4739

References

1. M.H. Brooker, O.F. Nielsen, E. Praestgaard. "Assessment of Correction Procedures for Reduction of Raman Spectra". J. Raman Spectrosc. 1988. 19(2): 71–78.
2. H. Aviv, I. Nemtsov, Y. Mastai, et al. "Characterization of Crystal Chirality in Amino Acids Using Low-Frequency Raman Spectroscopy". J. Phys. Chem A. 2017. 121(41): 7882–7888.
3. T. Koide, T. Fukami, H. Hisada, et al. "Identification of Pseudopolymorphism of Magnesium Stearate by Using Low-Frequency Raman Spectroscopy". Org. Process Res. Dev. 2016. 20(11): 1906–1910.
4. G. Walker, P. Römann, B. Poller, et al. "Pharmaceutical Mixtures During Milling: The Potency of Low-Frequency Raman Spectroscopy in Identifying Disorder". Mol. Pharm. 2017. 14(12): 4675–4684.
5. P.J. Larkin, M. Dabros, B. Sarsfield, et al. "Polymorph Characterization of Active Pharmaceutical Ingredients (APIs) Using Low-Frequency Raman Spectroscopy". Appl. Spectrosc. 2014. 68(7): 758–776.
6. I. Noda. "Two-Dimensional Infrared Spectroscopy". J. Am. Chem. Soc. 1989. 111(21): 8116–8118.
7. I. Noda. "Two-Dimensional Infrared (2D IR) Spectroscopy: Theory and Applications". Appl. Spectrosc. 1990. 44(4): 550–561.
8. I. Noda. "Generalized Two-Dimensional Correlation Method Applicable to Infrared, Raman, and Other Types of Spectroscopy". Appl. Spectrosc. 1993. 47(9): 1329–1336.
9. I. Noda, A.E. Dowrey, C. Marcott. "Recent Developments in Two-Dimensional Infrared (2D IR) Correlation Spectroscopy". Appl. Spectrosc. 1993. 47(9): 1317–1323.
10. I. Noda, Y. Ozaki. Two-Dimensional Correlation Spectroscopy: Applications in Vibrational and Optical Spectroscopy. Chichester, UK: John Wiley and Sons, 2004.

11. M. Perrot, M.H. Brooker, J. Lascombe. "Raman Light Scattering Studies of the Depolarized Rayleigh Wing of Liquids and Solutions". J. Chem. Phys. 1981. 74(5): 2787–2794.
12. G.E. Walrafen, M.R. Fisher, M.S. Hokmabadi, et al. "Temperature Dependence of the Low- and High-Frequency Raman Scattering from Liquid Water". J. Chem. Phys. 1986. 85(12): 6970–6982.
13. J.F. Rabolt. "Molecular Dynamics of a Crystal–Crystal Phase Transition in an Alternating Copolymer of Ethylene and Chlorotrifluoroethylene Using the Raman Active Longitudinal Acoustical Mode (LAM)". Polymer. 1981. 22(7): 890–895.
14. I. Noda. "Advances in Two-Dimensional Correlation Spectroscopy (2DCOS)". In: J. Laane, editor. Frontiers and Advances in Molecular Spectroscopy. Amsterdam: Elsevier, 2018. Ch. 2, Pp. 47–75.
15. M. Moskovits, K.H. Michaelian. "A Reinvestigation of the Raman Spectrum of Water". J. Chem. Phys. 1978. 69(6): 2306–2311.
16. K. Egashira, N. Nishi. "Low-Frequency Raman Spectroscopy of Ethanol−Water Binary Solution: Evidence for Self-Association of Solute and Solvent Molecules". J. Phys. Chem. B. 1998. 102(21): 4054–4057.
17. M.H. Brooker, M. Perrot. "Raman Studies of the Depolarized Rayleigh Wing of Liquids and Solutions". J. Mol. Struct. 1980. 60: 317–320.
18. I. Noda, P.R. Green, M.M. Satkowski, et al. "Preparation and Properties of a Novel Class of Polyhydroxyalkanoate Copolymers". Biomacromolecules. 2005. 6(2): 580–586.
19. B.J. Sobieski, I. Noda, J.F. Rabolt, et al. "Observation of Intermolecular Hydrogen Bonding Interactions in Biosynthesized and Biodegradable Poly[(R)-3-hydroxybutyrate-*co*-(R)-3-hydroxyhexanoate] in Chloroform and 1,1,1,3,3,3-Hexafluoro-2-propanol (HFIP)". Appl. Spectrosc. 2017. 71(10): 2339–2343.